International Journal of Heat and Fluid Flow 30 (2009) 117–130

Contents lists available at ScienceDirect

International Journal of Heat and Fluid Flow

journal homepage: www.elsevier.com/locate/ijhff

Intermittent spray cooling: A new technology for controlling surface temperature

Miguel R.O. Panão *, António L.N. Moreira

Technical University of Lisbon, Instituto Superior Técnico, IN+ Center for Innovation, Technology and Policy Research, Av. Rovisco Pais, 1049-001 Lisbon, Portugal

ARTICLE INFO

Article history:
Received 15 April 2008
Received in revised form 20 October 2008
Accepted 27 October 2008
Available online 6 December 2008

Keywords:
Spray cooling
Intermittent spray
Phase-Doppler
Heat transfer

ABSTRACT

In this work, intermittent spray cooling is proposed as a new technological concept to remove heat fluxes with good performance and introduce the potential use of advanced control techniques in the development of thermal management systems. The objective of this research work is to provide further insight into the physics involved in the heat transfer process triggered by the impact of an intermittent spray, and further investigate the effects of injection system parameters, such as the frequency of injection, pulse duration, initial wall temperature, pressure of injection and impingement distance, on the intermittent cooling system's performance. The results include a brief description of the spray intermittent behavior, an analysis on its thermal response and an evaluation of its performance. The "duty cycle", defined as the percentage of the cyclic time during which the cooling liquid is injected, is found to be the main parameter enabling a more accurate control of the cooling process. The experiments reported evidence that small duty cycles promote heat removal by phase-change. With larger duty cycles, the effect of reducing the time lag between consecutive injections is a greater interaction between cycles, eventually leading to the formation of a thin liquid film. As the duty cycle evolves toward the continuous spray condition, the cooling system's thermal response improves, but phase-change is mitigated, affecting the system's performance. Intermittent spray cooling is also compared with continuous spray cooling experiments and liquid savings has been estimated by 10–90% for the same energetic efficiencies reported in the literature. Finally, general guidelines are outlined for the design of thermal management systems based on intermittent spray cooling.

1. Introduction

There is a significant number of applications, such as the miniaturization of electronics in microprocessor developments, power electronics, high power amplifiers for radar systems, internal combustion engines, fire extinguishment, rapid cooling and quenching in metal foundries, ice chiller and air-conditioning systems, dermatologic surgery to name but a few, which demand for new cooling techniques capable of removing large heat dissipation rates. Among these new techniques, spray cooling appears to be one of the most notable methods with its ability for removing heat relying on phase-change, additionally to the convective heat transfer linked with fluid motion.

The two-phase flow generated in the spray cooling event has a highly complex nature and depends not only on several spray parameters, such as droplet size, velocity and density, but also on surface properties and morphology (e.g. roughness), and even on the initial surface temperature upon spray impact, therefore, it is difficult to clearly state which parameter is actually governing heat transfer (Panão and Moreira, 2006). Moreover, the fact that current spray cooling systems usually involve continuous sprays limits the control of heat dissipation rates to steady working conditions and their application in systems with transient cooling demands, such as in microelectronic devices, is a difficult task. In response to this limitation, an intermittent spray has been proposed and applied for two-phase cooling. In Moreira and Panão (2006), experiments were conducted using fuel injection technology for the spray intermittency and this new cooling concept was reported to remove heat at least as efficiently as continuous sprays, with the advantage of using lower overall mass fluxes.

An intermittent spray has the ability to provide a short timescale response in the control of heat fluxes by proper matching the frequency of injection with the pulse duration in the nucleate boiling heat transfer regime, according to the classical boiling theory. At low injection frequencies, nucleate boiling heat transfer is not limited by the delivery of liquid to the surface, or by the removal of vapor. At higher frequencies, an enhanced vaporization is induced by piercing and mixing the liquid film due to multiple drop impacts and a greater interaction between consecutive injections (Moreira and Panão, 2006). This ability for transient cooling is useful, for example, in microelectronic devices, where power dissipation rates depend on electronic current variations. In some cases,

Abbreviation: EGM, entropy generation minimization; ISC, intermittent spray cooling; LFS, leading front of the spray; PDI, phase-Doppler interferometer; SS, steady spray; ST, spray tail; TTL, transistor–transistor logic.

* Corresponding author. Tel.: +351 218417851; fax: +351 218496156.
E-mail address: mpanao@dem.ist.utl.pt (M.R.O. Panão).

0142-727X/$ - see front matter © 2008 Elsevier Inc. All rights reserved.
doi:10.1016/j.ijheatfluidflow.2008.10.005

Nomenclature

c_p	specific heat (J kg^{-1} K^{-1})
D	droplet diameter (μm)
DC	duty cycle $= \Delta t_{inj} f_{inj}^{-1} \times 100\%$ (%)
Ex, ex	exergy (J), specific exergy (J/kg)
f	frequency (Hz)
h	enthalpy (J kg^{-1})
h_{fg}	latent heat of evaporation (J kg^{-1})
k	thermal conductivity (W m^{-1} K^{-1})
L_w	plate thickness (mm)
$\dot{m}''$	mass flux (kg m^{-2} s^{-1})
p	pressure (bar)
$\dot{q}''$	heat flux (W m^{-2})
r_{disc}	disc radius (mm)
r_{tc}	thermocouple radius (mm)
T	temperature (°C)
t	time (s)
s	local specific entropy (J kg^{-1} K^{-1})
$\dot{S}''$	flux of entropy (W m^{-2} K^{-1})
U	droplet axial velocity (m s^{-1})
u	specific internal energy (J kg^{-1})
Z	axial distance (mm)

Greek letters

β	thermal effusivity (J m^{-2} K^{-1} s$^{-1/2}$)
χ	evaporated mass fraction
ϕ	irreversibility distribution ratio
Δt	time interval (ms)
ΔT	temperature difference (°C)
η_I	energy efficiency
η_π	exergy efficiency
μ	dynamic viscosity (kg m^{-1} s^{-1})
θ	top to bottom surface temperature difference
ρ	specific mass (kg m^{-3})
σ	surface tension (N m)
τ^*_{thr}	relative thermal response timescale $\xi = L_w \beta k_w^{-1}$ (s$^{1/2}$)

Subscripts

b	boiling point
c	convection
er	electric resistance
imp	impingement
in	impinging
inj	injection
gen	generated
p	primary
s	secondary
w	wall
wb	wall to boiling

the variation of heat dissipation rates may vary by orders of magnitude, which means that cooling time scales can be equal to, or less than 2 s (Cader et al., 2004). Therefore, the variable control of the cooling potential is an advantage of thermal management systems using intermittent sprays, providing an adequate response to eventual overall temperature variations by proper adjusting its cooling timescale.

In this work, intermittent spray cooling (ISC) is proposed as a new technological concept for meeting the challenge of transient heat dissipation requirements. The paper is structured as follows: After the present introduction, Section 2 further details the experimental method. Section 3 is dedicated to the results and their discussion, including: (i) a brief description of the spray intermittent behavior; (ii) an analysis on its thermal response, in order to understand, conceptually, how such system works; (iii) an evaluation of the spray cooling local performance for several frequencies, and durations of injection; (iv) the use of two fluids with different latent heat of evaporation for assessing the effect of this parameter; (v) and the last set of results reports preliminary studies on the parametric influence of the pressure of injection, impingement distance and initial surface temperature on the spray cooling performance. Finally, Section 4 summarizes the main conclusions and suggests some general guidelines for the optimization of an intermittent spray cooling system.

2. Experimental method

2.1. Experimental apparatus

The flow configuration is that of a spray striking perpendicular onto a flat aluminum disc with a 10 mm radius (r_{disc}), heated by an electric resistance coupled with a copper plate for uniformly distributing heat to the disc. The injector is a BOSCH pintle-type with 0.79 mm of pintle diameter inserted in a hole with 0.9 mm and the spray produced has a hollow-cone structure. The use of such structure instead of a full-cone spray follows previous experimental work where the potential advantages of the pattern produced by a hollow-cone spray were explored (Moreira and Panão, 2006). Nevertheless, the results and thermofluid dynamic analysis in this paper is locally developed and could be further extrapolated, with care, to full cone sprays. The fluid is supplied to the injector by a 2 L tank pressurized with N_2 and its temperature is 22 ± 2° C.

The injection frequency, pulse duration and number of injections are software controlled by a NI5411 arbitrary function generator from National Instruments. Two liquids were used in this experiment: HFE-7100 and acetone. Their thermophysical properties are listed in Table 1: specific mass (ρ); dynamic viscosity (μ); surface tension (σ); boiling temperature (T_b); liquid specific heat (c_p); and latent heat of vaporization (h_{fg}). The variation of HFE-7100 properties with temperature is provided by the manufacturer (3 M) and the properties of acetone were estimated according to Reid et al. (1986).

Three "Medtherm" eroding-K-type thermocouples were assembled in the disc, spaced by 4 mm (r_{tc}) with the first thermocouple located at the disc centre as depicted in Fig. 1. Thermocouple' signals are sampled at 50 kHz with a NI6024E National Instruments DAQ board plus a BNC2120, and the electrical signal is amplified with a gain of 300 before being processed to obtain surface tem-

Table 1
Fluids thermophysical properties.

Fluid (22 °C)	HFE-7100	Acetone
ρ (kg/m^3)	1488	790
μ (kg/m/s)	5.7×10^{-4}	3.2×10^{-4}
σ (mN m)	13.6	23.7
c_p (J/kg/K)	1177	2161
T_b (°C)	61	56.3
h_{fg} (kJ/kg)	111.6	534
s_L (295 K) (kJ/kg)	0.2632	2.005
s_V (T_b) (kJ/kg)	0.7474	3.344
h_L (295 K) (kJ/kg)	69.26	−3685.1
h_V (T_b) (kJ/kg)	223.2	−3297.6

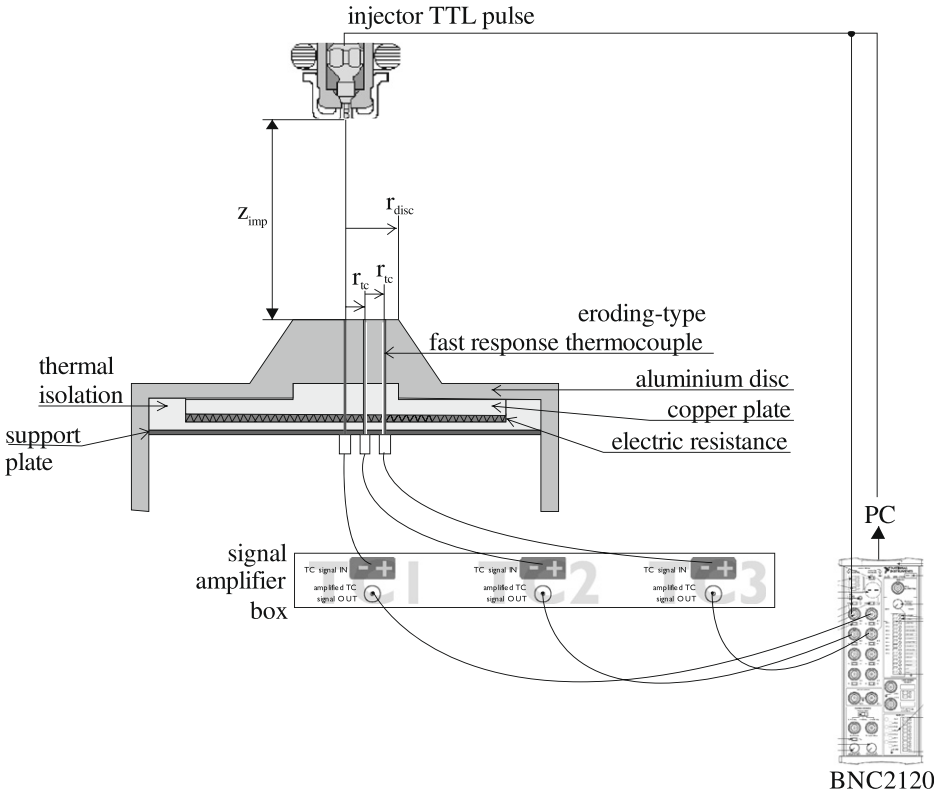

Fig. 1. Experimental setup scheme.

perature values. Inaccuracies due to electronic noise were inversely proportional to the surface temperature and represent an uncertainty smaller than ±1% (for a detailed analysis see Moreira and Panão, 2006).

Table 2 contains all the case studies used in this work. In each case, 100 series of 40 injection cycles were performed for averaging purposes.

Local time-resolved measurements of droplet size and velocity are simultaneously made at 3 mm above the surface, with a two-component phase Doppler interferometer (PDI) DANTEC system consisting of a 55X transmitting optics, a 57 × 10 PDI receiving optics, oriented at 30° for maximizing the signal visibility with negligible variations of the refractive index, and a 58N10 Covariance processor. The droplets impinging on the wall are distinguished from those produced by secondary atomization mechanisms through the axial velocity component (U). A positive axial velocity indicates impinging droplets, otherwise, secondary droplets. The number flux of impinging droplets depends on the effective cross-section area of the PDI measurement volume, which is calculated according to Roisman and Tropea (2001), Panão and Moreira (2005), and the error propagation analysis in the mass flux calculations resulted in uncertainties of less than 10% for mass flux quantities.

2.2. Methods for heat transfer analysis

The analysis performed in this work for studying ISC as a new technological concept depends on: (i) *mass fluxes*, measured by the phase-Doppler technique; (ii) *wall heat flux*, determined from measurements of the surface temperature and; (iii) *local energy and exergy efficiencies*, which evaluate the local spray cooling performance. In other spray cooling research works, the evaluation of the system's performance is usually approached from the point of view of the first-law of thermodynamics. In this paper, we suggest that including the point of view of the second-law of thermodynamics in this evaluation – through an exergy analysis – can be very useful. The advantage provided by an exergy analysis is to pinpoint the mechanisms which destroy exergy the most, understand why and evaluate their influence on the outcome, thus providing a more clear physical understanding of how can we optimize a spray cooling system by maximizing the useful energy from the energy available. A short note is that the exergy analysis developed here is locally restricted to the spray impingement event. The next sub-section addresses the methods used for quantifying the instantaneous wall heat flux, the local entropy generation and, consequently, the local exergy efficiency.

Table 2
Working conditions used in the experiments.

Case	f_{inj} (Hz)	Δt_{inj} (ms)	p_{inj} (bar)	ΔT_{wb} (°C)	Z_{imp} (mm)	Fluid
1–16	10, 20, 30, 60	5, 7.5, 10, 15	3	43.7	50	HFE-7100
17–18	10	5, 10	4	43.7	50	HFE-7100
19–22	10, 30	5	3	43.7	30, 40	HFE-7100
23–26	10, 30	5	3	20, 70	30	HFE-7100
27–34	10, 20	5, 7.5, 10, 15	3	43.7	50	Acetone
35–38	30, 60	5, 10	3	43.7	50	Acetone

2.2.1. Instantaneous wall heat flux considering a heat source

A methodology has been formulated to calculate the instantaneous wall heat flux from surface temperature measurements and considering an imposed heat flux as an important boundary condition. It has been previously shown that lateral heat conduction can be neglected (for more details see Moreira and Panão, 2006), therefore, the problem is considered unidirectional. The experiments performed in this work consider the heat transfer across a finite slab heated by a constant heat source, $\dot{q}''_{er}$, for which the equation of energy is expressed by

$$\begin{cases} \dfrac{\partial\theta}{\partial t} = \left(\dfrac{k_w}{\beta}\right)^2 \cdot \dfrac{\partial^2\theta}{\partial z^2} + \dfrac{k_w}{L_w\beta^2}\dot{q}''_{er} \\ \theta(z,t) = [T_w(z,t) - T_w(L_w,0)] \\ \beta = \sqrt{\rho k c_p} \end{cases} \tag{1}$$

where T_w is the wall temperature, z is the spatial coordinate perpendicular to the wall, β is the thermocouple thermal effusivity, k_w is the wall thermal conductivity and L_w is the disc thickness. The following initial and boundary conditions are considered in the solution of Eq. (1)

$$\theta(z,0) = \underbrace{\theta(L_w,0)}_{=0} - \frac{\dot{q}''_{er}}{k_w}(L_w - z) \tag{2}$$

$$\dot{q}''(0,t) = -k_w\frac{\partial\theta(0,t)}{\partial z} \tag{3}$$

$$\frac{\partial\theta(L_w,t)}{\partial z} = -\frac{\dot{q}''_{er}}{k_w} \tag{4}$$

The term $\theta(L_w,0)$ on the initial condition (2) is null, and the boundary condition (4) for the imposed heat flux on the bottom surface assumes at $t = 0$ a linear the temperature profile along the z-axis. To solve the differential Eq. (1), Laplace transformations are applied and the final general solution is given by

$$\theta(z,s) = A\cdot e^{z\sqrt{s/(k_w/\beta)^2}} + B\cdot e^{-z\sqrt{s/(k_w/\beta)^2}} + \frac{\dot{q}''_{er}}{s^2}\left(\frac{L_w - z}{k_w} + \frac{k_w}{L_w\beta^2}\right) \tag{5}$$

From the Laplace transform of the initial condition (2) and boundary conditions (3) and (4), the solution of (5) at the wall ($z = 0$) is given by

$$\theta(0,s) = \frac{\dot{q}''(0,s)}{\beta\cdot\sqrt{s}}\coth(\xi\sqrt{s}) + \frac{\dot{q}''_{er}}{\beta\cdot s^{3/2}}\left(\frac{1}{\sqrt{s}}\left(\frac{1}{\xi} - \xi\right) + \frac{1}{s}\tanh\left(\frac{\xi}{2}\sqrt{s}\right) - \operatorname{csch}(\xi\sqrt{s})\right) \tag{6a}$$

with $\xi = \frac{L_w\cdot\beta}{k_w}$.

The equation above should now be explicitly expressed for $\dot{q}''(0,s)$ as

$$\dot{q}''(0,s) = \frac{\beta\cdot s\cdot\theta(0,s)}{\sqrt{s}}\tanh(\xi\sqrt{s}) - \dot{q}''_{er}\left(\frac{1}{s^{3/2}}\left(\frac{1}{\xi} - \xi\right)\tanh(\xi\sqrt{s}) + \frac{1}{s^2}(1 - \operatorname{sech}(\xi\sqrt{s})) - \operatorname{sech}(\xi\sqrt{s})\right) \tag{6b}$$

However, some of the terms in Eqs. (6a) and (6b) include trigonometric hyperbolic functions of the Laplacian variable $\sqrt{s}$. However, because $\sqrt{s}$ directly reflects the frequency of temperature variations at the top surface according to Chen and Nguang (2003), for values of the order of 0.5–1 kHz, such as in the present work, one can approximate the solution for $\dot{q}''(0,s)$ as being bounded by $\sqrt{s}\to\infty$. This has been verified using an example of a temperature variation function (within a certain ΔT) where the variation frequency (f) can be varied, $\theta(0,t) = \Delta T\sin(2\pi f\cdot t) - \xi\dot{q}''_{er}/\beta$, for which the Laplace Transformation is applied to obtain $\theta(0,s)$. If the limits in the trigonometric hyperbolic functions are determined when $\sqrt{s}\to\infty$, the explicit form for the wall heat flux from (6b) can be simplified into

$$\dot{q}''(0,s) = \beta\cdot s\cdot\theta(0,s)\frac{1}{\sqrt{s}} - \dot{q}''_{er}\left(\frac{1}{s^{3/2}}\left(\frac{1}{\xi} - \xi\right) + \frac{1}{s^2}\right) \tag{7}$$

Using Laplace transformed function in the previous example, $\theta(0,s)$, it is possible to assess when the relative difference between Eqs. (6b) and (7) becomes below, for example, 1%, and it is observed, for the range of variation frequency between 0.5 kHz and 1 kHz, that this is achieved at $\sqrt{s} = 4.5$, therefore, above that value the assumption $\sqrt{s}\to\infty$ is valid and Eq. (6b) can be simplified into (7). When the frequency of temperature variations is small, for example, in the absence of spray impact, such that $\sqrt{s}\to 0$, the limits of the ratios with exponential functions lead to $\dot{q}''(0,s) = \dot{q}''_{er}$, thus showing the consistency of the derivation above.

The convolution theorem is used to find the analytical solution of (7), which, after some mathematical manipulation, becomes

$$\begin{cases} \dot{q}''(0,t) = \frac{\beta}{\sqrt{\pi}}\int_0^t \frac{\partial\theta(0,\tau)}{\partial\tau}\cdot\frac{1}{\sqrt{t-\tau}}d\tau - \dot{q}''_{er}\left(t + \frac{2}{\xi}\sqrt{\frac{t}{\pi}}\right) \\ \xi = \frac{L_w\beta}{k_w} \end{cases} \tag{8}$$

It is noteworthy that the solution above for the case $\dot{q}''_{er} = 0$, reduces to that already derived by Reichelt et al. (2002) for semi-infinite slab in the absence of heat sources. Eq. (8) shows that the effect of $\dot{q}''_{er}$ over $\dot{q}''(0,t)$ increases for thin wall thicknesses ($L_w\to 0$) and as heat transfer unfolds in time. Furthermore, the numerical implementation of Eq. (8), in order to obtain the instantaneous surface heat transfer from the measured temperature data, follows the approach developed in Schultz and Jones (1973) allow obtaining the following final expression

$$\begin{cases} \dot{q}''(0,t_n) = \frac{2\beta_{t_n}}{\sqrt{\pi}\cdot\delta t}\sum_{i=1}^{n}\frac{\theta(0,t_i) - \theta(0,t_{i-1})}{\sqrt{n-i+1} + \sqrt{n-i+1}} - \dot{q}''_{er}\left(t_n + \frac{2}{\xi_{t_n}}\sqrt{\frac{t_n}{\pi}}\right) \\ \xi_{t_n} = \frac{L_w\beta_{t_n}}{k_w} \end{cases} \tag{9}$$

where $t_i = i\ \delta t$ and δt is the sampling time, or else the inverse of the sampling rate. It should be emphasized that the solution and implementation in Eq. (9) are only valid for a constant imposed wall heat flux ($\dot{q}''_{er} = \text{const}$).

2.2.2. Entropy generated flux

The analysis based on the second-law of thermodynamics is aimed at the evaluation of the exergy efficiency, which requires the knowledge of the entropy generation flux through heat and fluid flow in the spray cooling event.

The conservation of the mass flux (m'' in kg m^{-2}) and balances of specific energy (u in J kg^{-1}) and entropy flux (S'' in J m^{-2} K^{-1}) rates applied to the open system illustrating the spray cooling event, as depicted in Fig. 2, are expressed as

$$\frac{Dm''}{Dt} = \dot{m}''_{in} - \dot{m}''_{s} - \dot{m}''_{vap} \tag{10}$$

$$\rho\frac{Du}{Dt} = -\nabla\cdot\dot{q}'' - p(\nabla\cdot v) \tag{11}$$

$$\frac{DS''}{Dt} = \dot{m}''_{in}\cdot s_{in} - \dot{m}''_{s}\cdot s_s - \dot{m}''_{vap}\cdot s_V + \frac{\dot{q}''_w}{T_w} + \dot{S}''_{gen} \tag{12}$$

The term on the left hand side of Eq. (10), $\frac{Dm''}{Dt}$, is the mass flux which may accumulate on the surface and form a liquid film; and if we assume that the temperature of impinging drops, as well as the temperature of secondary drops are equal to the fluid temperature in ambient conditions, the specific entropies s_{in} and s_s are equal and, henceforth, referred as s_L. The terms on the right hand side of the energy conservation Eq. (11) are, respectively, the heat transferred by the spray cooling event, the work exerted by pressure forces on spray impaction, and it should be noted that the term associated with viscosity ($\mu\cdot\Phi$) is neglected in this work. In Eq. (12) relatively

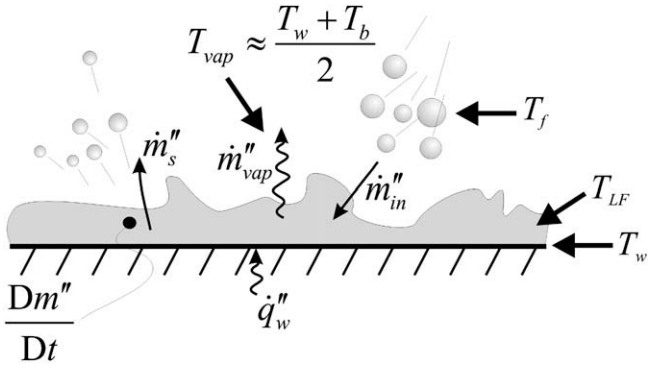

Fig. 2. This scheme illustrates intermittent spray cooling as an open thermodynamic system.

to the entropy balance on the spray cooling event, in its right hand side, the first three terms are associated with the entropy of incoming and outgoing mass fluxes, followed by a term associated with the entropy generated by the cooling event ($\dot{q}''_w$) at the wall temperature (T_w) which is a function of time and, henceforth, refers to the top surface at $z = 0$, and finally, the last term is the one we wish to estimate, the entropy generated flux ($\dot{S}''_{gen}$).

The fact that all experiments were performed at atmospheric pressure means the spray cooling event in the present analysis is an isobaric process, therefore, using the material derivative in the canonical relation for the internal energy $du = Tds - pd(1/\rho)$ one obtains

$$\rho \frac{Ds}{Dt} = \frac{\rho}{T}\frac{Du}{Dt} - \frac{p}{\rho T}\frac{D\rho}{Dt} \tag{13}$$

and after applying it to Eq. (11), the term associated with pressure forces is eliminated by the continuity equation, and further assuming a unidirectional heat conduction, the expression in (11) is simplified to

$$\frac{Ds}{Dt} = -\frac{1}{\rho T}\frac{\partial \dot{q}''}{\partial z} \tag{14}$$

Considering at the liquid–gas interface that the convective heat flux is $\dot{q}''_c = \dot{q}''_w + \frac{\partial \dot{q}''}{\partial z} dz$, and that $\dot{q}''_c \ll \dot{q}''_w$, then the heat flux gradient in Eq. (14) could be approximated by

$$\frac{\partial \dot{q}''}{\partial z} \approx -\frac{\dot{q}''_w}{h_f} \tag{15}$$

where dz is approximated by the dynamic film thickness h_f, and Eq. (14) simplifies into

$$\rho \frac{Ds}{Dt} \approx \frac{\dot{q}''_w}{T \cdot h_f} \tag{16}$$

with ρ as the density of the liquid–vapor mixture, given by $\rho = \chi\rho_V + (1-\chi)\rho_L$ and χ is the evaporated mass fraction. The temperature T is the mean temperature of an eventually formed liquid film, assumed as an average between the vapor temperature ($T_{vap} = (T_w + T_b)/2$) and that of the impinging droplets (T_f) as $T_{LF} = 0.5(T_{vap} + T_f)$.

In order to resolve the left hand side of Eq. (16), one takes the volumetric entropy in the control volume expressed as $S''' = \rho \cdot s$, applies to it the material derivative (D/Dt) and resolves in order of $\rho Ds/Dt$, considering negligible the variation of ρ_V with time and that $\rho_L = h_f^{-1} Dm''/Dt$, results in

$$\rho \frac{Ds}{Dt} = \frac{DS'''}{Dt} - \frac{(1-\chi)\cdot s}{h_f}\frac{Dm''}{Dt} \tag{17}$$

where the volumetric entropy is $S''' = S''/h_f$ and $s = \chi s_V + (1-\chi)s_L$ is the specific entropy of the two-phase flow inside a liquid film under the nucleate boiling regime. Therefore, conjugating (16) with (17), results in a simplified version of (11) in the form

$$\frac{DS''}{Dt} = \left[(\chi - \chi^2)s_L + (1-\chi)^2 s_V\right]\frac{Dm''}{Dt} + \frac{\dot{q}''_w}{T_{LF}} \tag{18}$$

where it is recalled that χ is the mass fraction of evaporated liquid, s_L and s_V are the specific entropies of liquid and vapor, respectively, Dm''/Dt is the mass flux deposited on the wall and T_{LF} is the temperature of an eventually formed liquid film.

If Eqs. (10) and (18) are introduced in (12), additionally with the simplification for the evaporated mass flux as a fraction (χ) of the difference between the mass fluxes of incoming impinging drops and outgoing secondary droplets as $\dot{m}''_{vap} = \chi(\dot{m}''_{in} - \dot{m}''_s)$, after some mathematical manipulation an expression is derived to estimate the entropy generated flux in $W\,m^{-2}\,K^{-1}$ as

$$\dot{S}''_{gen}(\chi) = [\varphi_L(\chi)s_L + \varphi_V(\chi)s_V]\Delta\dot{m}'' + \dot{q}''_w\left(\frac{1}{T_{LF}} - \frac{1}{T_w}\right)$$
$$\begin{cases} \varphi_L(\chi) = \chi(3\chi - \chi^2 - 3) \\ \varphi_V(\chi) = \chi(\chi^2 - 2(\chi - 1)) \\ \Delta\dot{m}'' = \dot{m}''_{in} - \dot{m}''_s \end{cases} \tag{19}$$

2.2.3. Irreversibility mechanisms in spray cooling

The application of the second-law of thermodynamics to spray cooling is only useful if it leads to a better understanding of the reasons underlying exergy losses and how to optimize the cooling process. In this sense, it should be emphasized that the formalism of the local entropy generated flux contains two irreversibility mechanisms associated with

(i) The evaporated mass flux: $\dot{S}''_{gen,\Delta\dot{m}''}(\chi) = [\varphi_L(\chi)s_L + \varphi_V(\chi)s_V]\Delta\dot{m}''$.
(ii) The wall heat flux removed by the impinging spray: $\dot{S}''_{gen,\dot{q}''_w} = \dot{q}''_w\left(\frac{1}{T_{LF}} - \frac{1}{T_w}\right)$.

If the entropy generation minimization (EGM) method is applied to these irreversibility production mechanisms, it is possible to find thermodynamic optima suggesting the condition which leads the process to work with the best performance (Bejan, 1996).

Relatively to the entropy generated by the evaporated mass flux, the optimal parameter is the fraction of evaporated mass χ. The optimal value is found by taking the derivative of Eq. (19) with respect to χ, setting it equal to zero, and solving for the evaporated mass fraction, thus resulting in

$$\chi_{opt} = \frac{3s_L - 2s_V - \sqrt{3s_L s_V - 2s_V^2}}{3(s_L - s_V)} \tag{20}$$

which requires a positive term inside the square root, such that $s_L \geqslant \frac{2}{3}s_V$. The equality in the former expression sets the lower limit optimal value, $\chi_{opt} = 0$. The upper-limit of the inequality is $s_L \to s_V$, which could only occur near the critical temperature of the cooling liquid and implies that only half of impinging mass is vaporized ($\chi_{opt} = 0.5$). This analysis indicates that exergy losses should be minimum if the cooling liquid vaporization is minimized, favoring the presence of a liquid film on the surface, as in some continuous spray cooling concepts (see Pautsch and Shedd, 2005; Shedd and Pautsch, 2005).

The application of the EGM method to the second irreversibility production mechanism associated with the wall heat flux (which should be as high as possible), leads the search for optimal parameters in the temperatures involved. The derivative of Eq. (19) produces only a solution for the optimization of the wall temperature

as $T_{w,\mathrm{opt}} = T_b + 2T_f$, which can be interpreted with respect to the superheating degree ($\Delta T_{wb,\mathrm{opt}} = T_{w,\mathrm{opt}} - T_b$) as

$$\Delta T_{wb,\mathrm{opt}} = 2T_f \tag{21}$$

This simple criterion based on the least production of irreversibilities in the system is technically interesting for choosing the most adequate fluid in the optimal design of a certain spray cooling application. It should be stressed that the optimal wall temperature corresponds to the working temperature of the heat dissipating surface, which the spray cooling system is required to maintain at a constant value. An example of the application of this criterion is to consider a cooling system requiring the maintenance of the surface temperature of a microprocessor at 80 °C using a dielectric fluid. If HFE-7000 is used, the cooling liquid boiling temperature (T_b) is 34 °C, and according to the criterion in Eq. (21), the fluid temperature should be at 23 °C, which is value close to typical working environments. However, if HFE-7100 is used instead, the fluid temperature (T_f) should be at 9.5 °C, which is inadequate because it demands a high sub-cooling degree of the liquid injected.

In the present work, most experiments summarized in Table 2 were performed with a superheating degree ΔT_{wb} of 43.7 °C, therefore, according to the criterion in Eq. (21), the fluid temperature should be ≈22 °C to ensure the minimum production of irreversibilities, which is the value reported in the experimental setup (Section 2.1). As will be shown later when analyzing the preliminary parametric studies on the effect of ΔT_{wb} relatively to the exergy efficiency, the best performance is actually obtained when this criterion is fulfilled (Section 3.4, Fig. 13).

The interpretations above based on the application of the EGM method apparently pose to the designer a certain paradox. While it is suggested that the best spray cooling performance is obtained in the presence of a liquid film, which is known to inhibit liquid evaporation by mitigating (not suppressing) phase-change, it is also important to maximize the wall heat flux, through the promotion of phase-change and, paradoxically, avoid the formation of a liquid film. For this reason, the relative importance between both irreversibility production mechanisms should be carefully evaluated and, consequently, it is more useful to express the entropy generated flux as

$$\dot{S}''_{\mathrm{gen}} = (1+\phi)\dot{S}''_{\mathrm{gen},\dot{q}''_w}$$
$$\phi = \frac{\dot{S}''_{\mathrm{gen},\Delta\dot{m}''}}{\dot{S}''_{\mathrm{gen},\dot{q}''_w}} \tag{22}$$

where ϕ is the irreversibility distribution ratio.

Since χ is an arbitrary quantity between 0 and 1, for the purpose of analysis, the entropy generated flux is integrated over this range, which means that irreversibilities produced by mass flux differences are given by

$$\dot{S}''_{\mathrm{gen},\Delta\dot{m}''}\chi = \int_0^1 \dot{S}''_{\mathrm{gen},\Delta\dot{m}''}\mathrm{d}\chi = 12^{-1}(7s_L - 9s_V)\cdot\Delta\dot{m}'' \tag{23}$$

2.2.4. Exergy efficiency for evaluating intermittent spray cooling local performance

It is well known that energy conserves itself, while exergy can be destroyed. The destruction of exergy implies the destruction of the energetic potential for spray cooling due to thermodynamic irreversibilities. In the former section, these irreversibilities have been identified with the evaporation of mass and the wall heat flux. In this section, the local exergy efficiency is formulated to evaluate the system's performance in destroying as little available cooling potential as possible, i.e. the exergetic efficiency usefulness is to assess which working conditions ensure the best possible

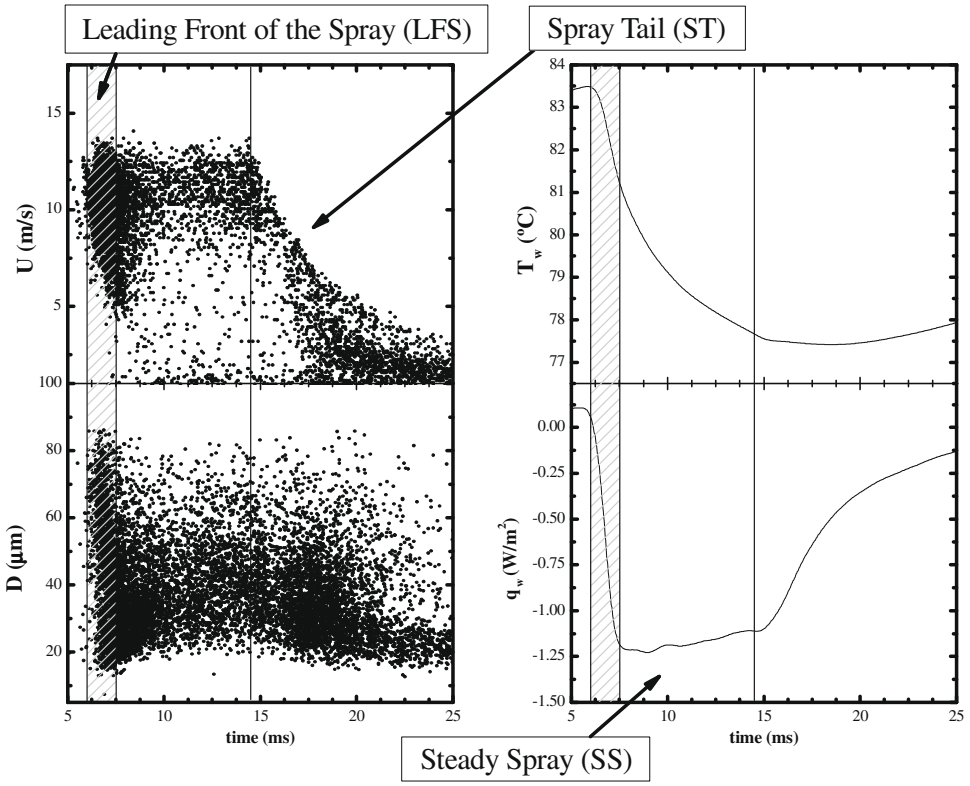

Fig. 3. On the left, the plots correspond to the axial velocity (U) and size (D) of impinging drops. On the right, the plots correspond to the simultaneous measurement of the wall temperature (T_w) and the calculated instantaneous wall heat flux ($\dot{q}''_w$) considering a total of 200 series of 40 injections each, for a spray injecting at 20 Hz with pulse duration of 10 ms. The several periods of the spray dynamic behavior are also indicated.

quality of the system's cooling potential. In this context, it should be noted that the analysis based on the second-law of thermodynamics is solely focused on the impingement control volume between the solid–liquid and liquid–gas interfaces, excluding other elements of the experimental setup, such as the exergy associated with the opening and closing of the injector.

The balance of exergy in the control volume depicted in Fig. 2 and used in the previous section is written as

$$\frac{\mathrm{D}Ex''}{\mathrm{D}t} = \left(1 - \frac{T_0}{T_w}\right)\dot{q}''_w + \dot{m}''_{\mathrm{in}} ex_{\mathrm{in}} - \dot{m}''_s ex_s - \dot{m}''_{\mathrm{vap}} ex_V - T_0 \dot{S}''_{\mathrm{gen}} \quad (24)$$

with Ex'' as the exergy flux, T_0 is the reference temperature considered here as the fluid temperature T_f and ex is the specific exergy, where an equal value is assumed between impinging and secondary droplets, $ex_{\mathrm{in}} = ex_s = ex_L$. The first two terms on the right hand side of Eq. (24) correspond to the inlet exergy flux, and the two that follow to the outlet exergy allowing to re-write Eq. (24) as $\frac{\mathrm{D}Ex''}{\mathrm{D}t} = E\dot{x}''_{\mathrm{in}} - E\dot{x}''_{\mathrm{out}} - T_0\dot{S}''_{\mathrm{gen}}$ from which the exergy efficiency can be deduced as

$$\eta_{\Pi} = 1 - \frac{\frac{\mathrm{D}Ex''}{\mathrm{D}t} + T_0\dot{S}''_{\mathrm{gen}}}{E\dot{x}''_{\mathrm{in}}} \quad (25)$$

All the elements in Eq. (25) can be obtained from experimental evidence and more details on how each element is calculated can be found in Appendix A.

3. Results and discussion

Intermittent spray cooling depends intrinsically on the dynamic behavior of the impinging spray, which is first analyzed in this section. Following, the thermal response of the cooling system is evaluated taking into account the parameters defining the spray intermittency. Afterwards, the local performance of intermittent spray cooling is analyzed based on the energy and exergy efficiencies. And finally, a preliminary study is made on the influence of other parameters affecting the system's cooling performance, such as superheating degree, impingement distance and pressure of injection.

3.1. Spray intermittent behavior

To exemplify the spray dynamic behavior, simultaneous measurements of droplet size, velocity, phase-average surface temperature and wall heat flux are depicted in Fig. 3 considering a total of 200 series of 40 injections each, for a spray injecting at 20 Hz with pulse duration of 10 ms. The correlation between the dynamic behavior of the spray and the surface thermal behavior is evident in the plots, which is why synchronized measurements of the droplets characteristics and surface cooling are necessary if the two are to be accurately correlated (Loureiro et al., 2004; Moreira et al., 2007). In Panão and Moreira (2006), the spray dynamic behavior was correlated with heat transfer in three time-dependent regimes (Fig. 3).

The first regime occurs during the *leading front of the spray* period (LFS). It lasts for 0.75–1 ms after the first droplets hit the surface and is characterized by intense size and velocity gradients of droplets impinging on the wall, producing a similar gradient of the wall heat flux. In this regime, heat transfer depends mainly on the number flux of droplets, a result equally observed by Yao and Choi (1987), Estes and Mudawar (1995) and Pautsch and Shedd (2005) for continuous sprays.

The second time-dependent regime occurs during the *steady spray* period (SS). It is characterized by a *quasi*-steady behavior of the spray, as well as in the heat flux removal and lasts until the end of injection. Previous work has shown that heat transfer in this period is mainly governed by variations of the mean droplet size (Panão and Moreira, 2005).

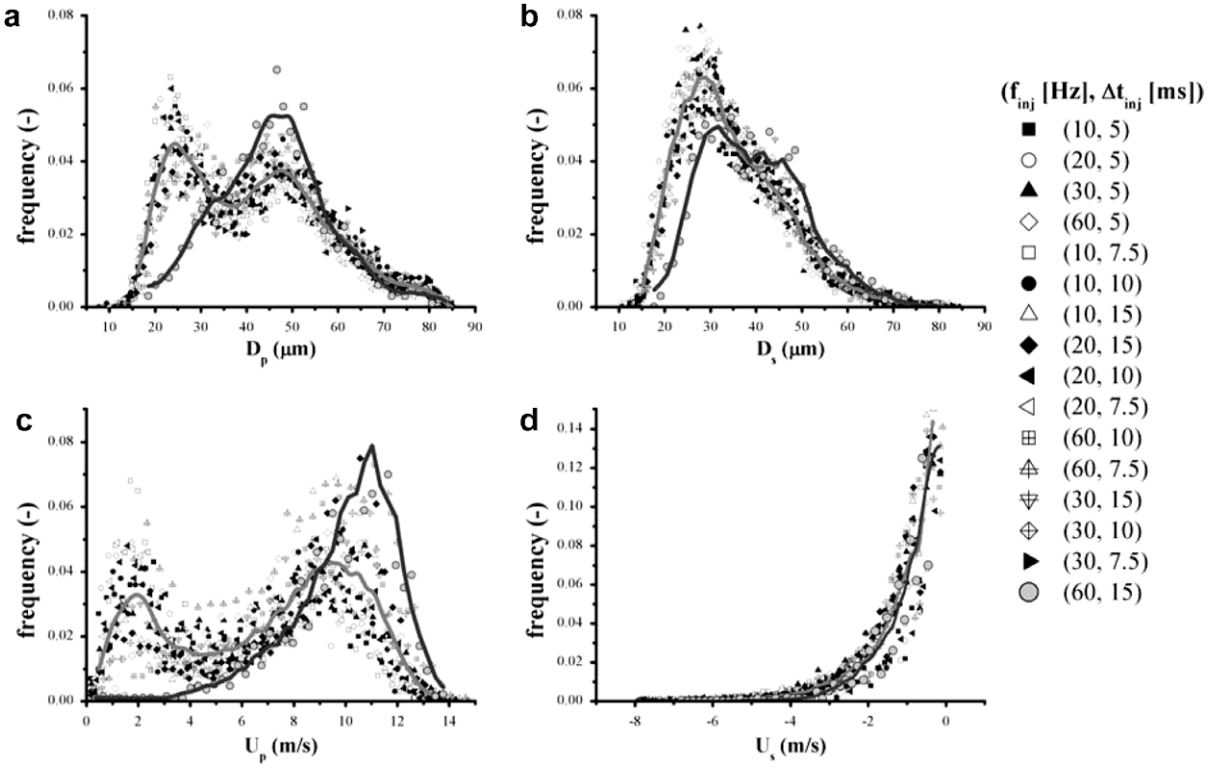

Fig. 4. PDF's for the several frequencies of injection (f_{inj} [Hz]) and pulse durations (Δt_{inj} [ms]) with HFE-7100: (a) size of impinging droplets; (b) size of secondary droplets; (c) axial velocity of impinging droplets; (d) axial velocity of secondary droplets.

The third and final time-dependent regime is the *spray tail* period (ST) during which droplet velocity and heat transfer decrease monotonically. Previous work (Panão and Moreira, 2006) has shown that heat transfer in this regime is correlated with the axial velocity of impinging droplets (see also Arcoumanis and Chang, 1993).

The question which now arises is whether the spray characteristics are affected or not by the injection frequency or pulse duration and the answer is no. In terms of the size and axial velocity distributions of impinging and secondary droplets, shown in Fig. 4, neither the injection frequency nor pulse duration produce significant changes in the bimodal shape of the PDF represented by the gray average line. The reason for being bimodal is due to the re-entrainment of secondary droplets in the time interval between the end of injection and the start of next injection cycle. This re-entrainment is induced by the vortical structures formed after impact, which drag these smaller and more responsive droplets, leading to their eventual re-impact on the surface in the period between the closing of the injector pintle and the start of the next injection event (Panão and Moreira, 2004). The discrete probability distribution different from the remaining correspond to an injection frequency of 60 Hz and a 15 ms pulse duration, meaning the injection of cooling liquid for 90% of the cycle time, which is close to the working condition of a continuous spray (injecting for 100% of the cycle time), therefore, this case can reasonably represent how an ISC system would work in a continuous spray cooling mode.

It should be noted that secondary droplets are mainly produced by hydrodynamic impact mechanisms (rebound and splash). However, when the spray impact occurs on heated surfaces, and a thin/short-duration liquid film eventually forms by the interaction between consecutive injection cycles, an additional secondary atomization mechanism emerges by thermal induced heat transfer effects consisting in the disruption of bubbles at the liquid–air interface (Moita and Moreira, 2007). This is evidenced in the images of Fig. 5 where more secondary droplets are observed when the DC increases up to 90%. In this way, Fig. 5 depicts the result of a greater interaction observed between consecutive injections, i.e. the reduction of the time lag between consecutive injection events, eventually leading to the formation of a thin liquid film.

The fact that in this ISC system, the impinging spray remains relatively the same for the cases 1–16 listed in Table 2, as depicted in Fig. 4, allows concluding that any variations of the surface temperature is due to the heat transfer occurring at the impaction site and not caused by any changes in the spray dynamics prior to its impact (exemplified in Fig. 6 for several duty cycles keeping the pulse duration at 5 ms). Further information on the mass flux of impinging and secondary droplets measured by the phase-Doppler diagnostic system is systematized in Table 3. This data will be later used in the calculation of energy and exergy efficiencies.

3.2. Thermal response during intermittent spray cooling

Spray cooling systems seek the best thermal response possible. However, in intermittent spray cooling there is an additional potentiality of *control*. This is one of the main advantages of this technological concept, i.e. provide a system with a reliable control over the thermal responsiveness by proper matching the frequency with the duration of injection. The relation between these two parameters can be expressed by the "duty cycle" (DC), defined as a percentage of the cycle time ($1/f_{inj}$) during which the cooling liquid is injected (Δt_{inj}): DC = $\Delta t_{inj} f_{inj} \times 100\%$. There are two obvious ways of changing DC, either by increasing the frequency and keeping the pulse duration constant (as in Majaron et al., 2002), or vice-versa.

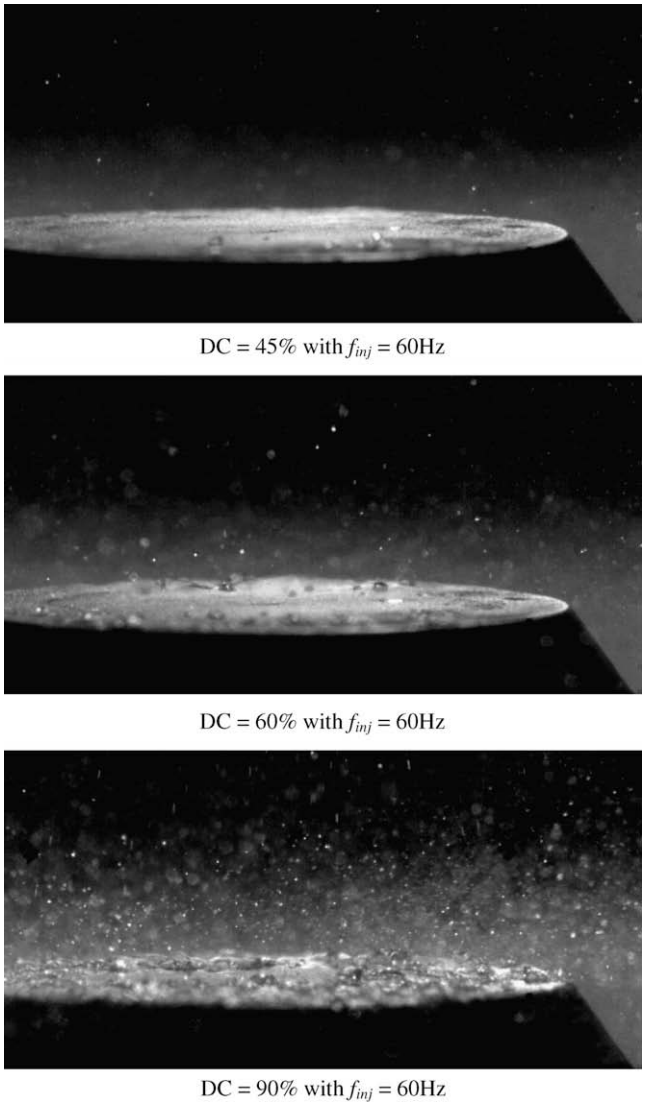

Fig. 5. These images correspond to experiments using HFE-7100 at 18 ms after the impact moment of the last in a series of 40 injections cycles. The frequency of injection is maintained at 60 Hz and the duty cycle is change by a proper match of the pulse duration.

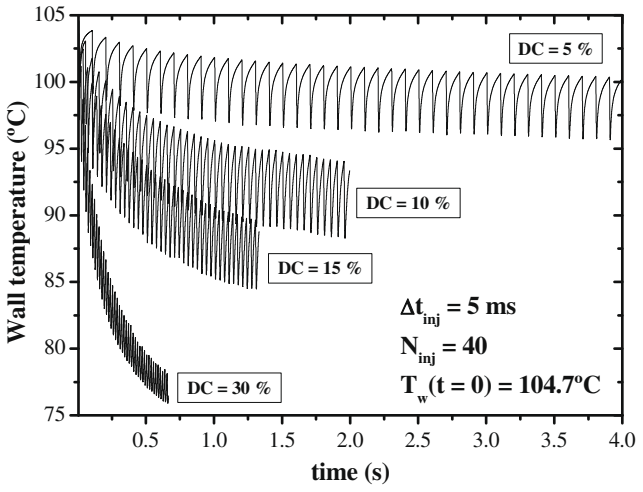

Fig. 6. Evolution of the wall temperature for several duty cycles keeping the pulse duration at 5 ms.

Table 3
Mass fluxes for impinging and secondary droplets measured by the phase-Doppler system.

T_w (t = 0) (°C)	f_{inj} (Hz)	DC (%)	z_{imp} (mm)	p_{inj} (bar)	$\dot{m}''_{in} \times 10^4$ (kg s^{-1} cm^{-2})	$\dot{m}''_{out} \times 10^4$ (kg s^{-1} cm^{-2})
HFE-7100						
81	10	5	30	3	0.39837	0.02237
104.7					0.23572	0.02393
131					0.30946	0.03730
81	30	15			0.82970	0.08871
104.7					0.77722	0.05975
131					1.17771	0.09034
104.7	10	5	40	3	0.24891	0.10580
	30				0.76479	0.22240
	10	5	50	4	0.13779	0.01334
		10			0.36930	0.03481
	10	5	50	3	0.09824	0.01468
		7.5			0.19505	0.07519
		10			0.26653	0.09052
		15			0.45806	0.18825
	20	10			0.30109	0.18059
		15			0.53875	0.22029
		20			0.53207	0.32063
		30			1.07151	0.56424
	30	15			0.88293	0.20083
		22.5			0.43785	0.05996
		30			1.15404	0.45911
		45			0.81957	0.17924
	60	30			0.94714	0.27453
		45			0.86741	0.35550
		60			1.19786	0.50303
		90			0.74256	0.08935
Acetone						
100	10	5	30	3	0.02975	n.a.
	30	15			0.03815	n.a.
	10	5	40		0.03687	n.a
	30	15			0.12150	n.a.
	10	5	50	4	0.08466	0.00199
		10			0.09281	n.a
	20	10			0.10877	n.a.
	10	5		3	0.11836	0.00444
		7.5			0.06361	n.a.
		10			0.22512	0.01608
		15			0.10297	n.a.
	20	10			0.19306	0.01107
		15			0.24264	0.00367
		20			0.27176	0.00099
		30			0.31439	n.a.
	30	15			0.25674	0.01086
		30			0.16495	n.a.
	60	30			0.53673	0.03658
		60			0.25214	n.a.

Note: n.a. is a non available value considered zero in the calculations, meaning a negligible mass flux of secondary droplets.

In this section, the relation between DC and the systems thermal responsiveness is investigated. The results presented in this analysis correspond to the cooling liquid HFE-7100, and the thermal response is here evaluated by the decay of the initial temperature of each injection along a number of consecutive cycles (#40). Fig. 7 shows the temperature decays of the initial temperature of each injection cycle, averaged over 1 ms before the electronic start of injection. In each plot, the pulse duration is fixed and the injection frequency increases from 10 Hz to 60 Hz. The DC value in each case is also indicated.

As DC increases, the results show an improvement of the system's thermal response, as well as a larger cooling power, indicated by the increasingly larger difference between the surface temperature before the first and the last injection cycles. This suggests the system's ability of changing its cooling potential just by adequately adjusting the DC, e.g. a larger DC implies a faster and more powerful cooling of the surface, although limited to the system's cooling at DC = 100%.

It should be noted that the same DC, for example of 15%, can be obtained with three different matches of pulse duration and injection frequency: (i) a 5 ms pulse with 30 Hz; (ii) a 7.5 ms pulse with 20 Hz; (iii) or else, a 15 ms pulse duration with 10 Hz. For the working conditions used in these experiments, Fig. 8 shows similar temperature decays with equal DC values, indicating the duty cycle as the determining parameter in intermittent spray cooling.

In order to evaluate the system's thermal response as a function of DC, a timescale is defined as the ratio between the time interval that each condition took to reach the lowest temperature decay ($\Delta T_{N_{inj}}$) obtained from all the experiments (e.g. $(\min \Delta T_{N_{inj}}) = 3.34$ °C with HFE-7100, at 10 Hz and DC = 5%), and the corresponding time interval for that condition (δt of $(\min \Delta T_{N_{inj}}) = 3.9$ s with HFE-7100):

$$\tau^*_{thr} = \frac{\delta t \text{ at } \min(\Delta T_{N_{inj}})}{\delta t \text{ of } \min(\Delta T_{N_{inj}})} \tag{26}$$

The results depicted in Fig. 9 show the non-linear correlation between the relative thermal response timescale as DC increases and approaches the condition equivalent to a continuous spray (DC = 100%).

The practical significance of these results is the clear advantage of intermittent spray cooling to control the timescale of the system's thermal response by properly adjusting its duty cycle. This opens spray cooling technology to the potential use of intelligent control strategies in the future, e.g. neural networks, as highly sophisticated ways of accurately control the cooling process. In the following section, the effect of varying DC in the system's performance is evaluated by the energy and exergy efficiencies.

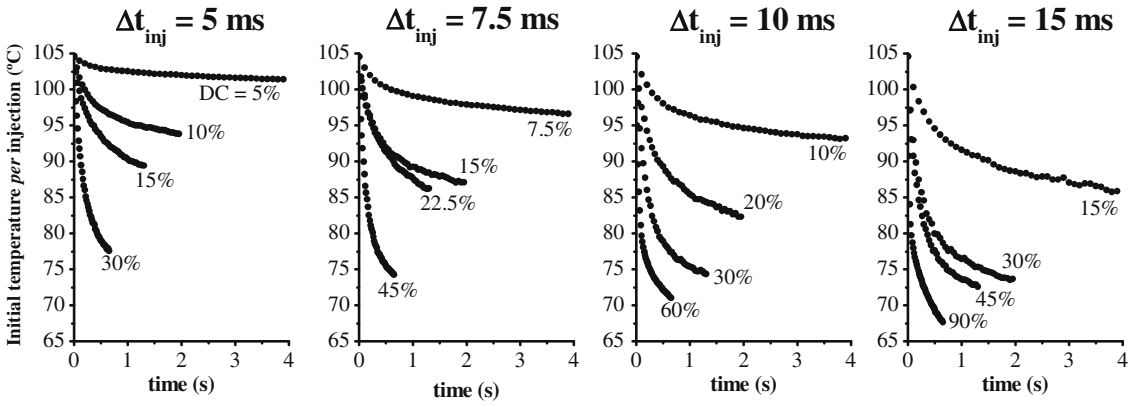

Fig. 7. Surface temperature decays along the series of consecutive injection cycles at different duty cycles (DC) values keeping the pulse duration constant.

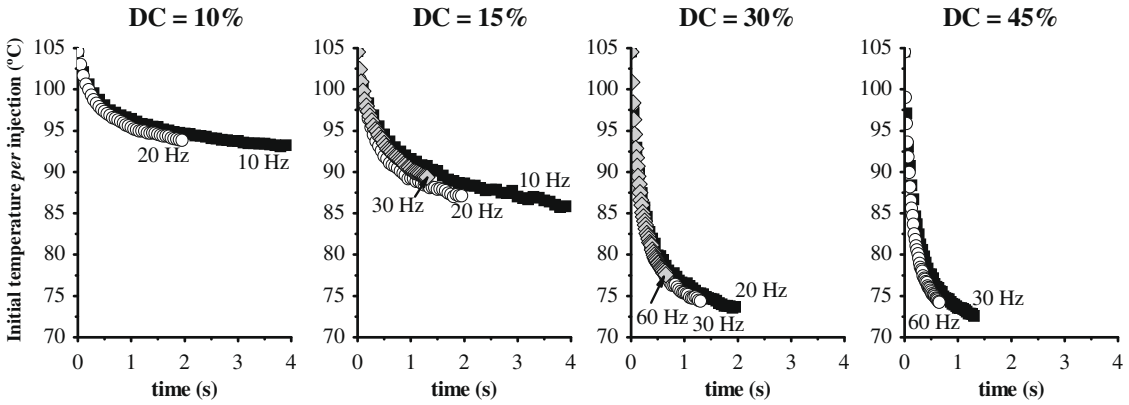

Fig. 8. Surface temperature decays along the series of consecutive injection cycles of several cases with the same duty cycle (DC), for experiments with HFE-7100.

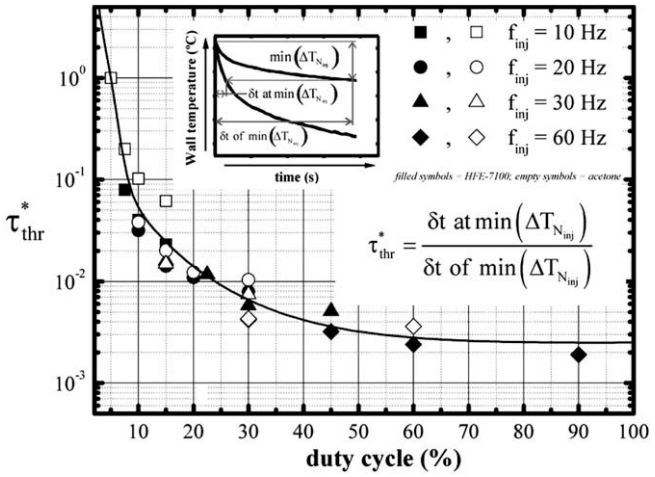

Fig. 9. Effect of the duty cycle (DC) in the thermal response timescale of both HFE-7100 and acetone.

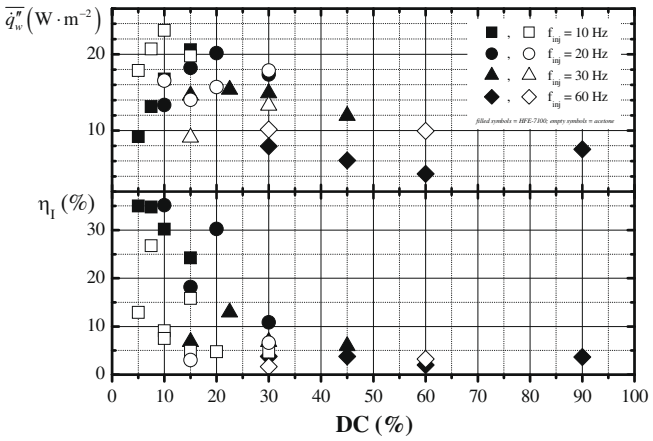

Fig. 10. Time-average wall heat flux (top) and energy efficiency (bottom) as function of the duty cycle (DC) for HFE-7100 and acetone.

3.3. Evaluation of intermittent spray cooling local performance

The local cooling performance of an intermittent spray impact is evaluated for each experimental condition by a joint analysis of the energy and exergy efficiencies. The energy efficiency is determined by

$$\eta_I = \frac{\overline{\dot{q}''_w}}{G \cdot (c_p \Delta T_{bf} + h_{fg})} \qquad \begin{cases} G = N_{\mathrm{inj}} \mathrm{D}m''/\mathrm{D}t \\ \overline{\dot{q}''_w} = \frac{1}{T(N_{\mathrm{inj}})} \int_0^{T(N_{\mathrm{inj}})} \dot{q}''_w(t)dt \end{cases} \tag{27}$$

where N_{inj} is the number of injection cycles in each series, G is the mass flux deposited on the heated surface expected to vaporize completely and $\overline{\dot{q}''_w}$ is the average wall heat flux. If we depict the energy efficiency and the time-average wall heat flux as a function of DC (Fig. 10), the results show that intermittent spray cooling is more efficient and extracts more heat with lower duty cycles. Also, the trend observed is a decrease of the system's efficiency as DC increases toward 100%, i.e. to the system injecting continuously. An important outcome of these results is the evidence that an intermittent spray can perform better than a continuous spray.

Even though with smaller DCs an intermittent spray cooling performs better than a continuous spray, this should be analyzed jointly with the quality of this cooling potential, which is given by the exergy efficiency calculated through Eq. (25), based on the time-averaged entropy generated flux, $\overline{\dot{S}''_{\mathrm{gen}}} = \frac{1}{T}\int_0^T \dot{S}''_{\mathrm{gen}}(t)\mathrm{d}t$, assuming a quasi-static condition in each ∂t, i.e. an equilibrium state, and the average wall heat flux in Eq. (27). For the dielectric fluid (HFE-7100), the evolution of the energy efficiency with DC, observed in Fig. 10, is followed by a decrease in the quality of the cooling potential toward the working mode of a continuous spray (DC = 100%), as depicted in Fig. 11. However, this is quite different if acetone is used instead (open symbols). The reason for this difference can be further explored by analyzing the irreversibility distribution ratio defined in (22), ϕ, which expresses the relative importance between the irreversibilities produced by the evaporated mass of cooling liquid and those produced by the heat flux extracted from the wall (Fig. 12).

The irreversibility distribution ratio ϕ in the experiments with HFE-7100 and duty cycles below 25%, inform us of a clear dominance of the irreversibility produced by the wall heat flux, which is apparently correlated with high exergy efficiency values. However, once $\phi > 1$, it means the evaporation of mass becomes the dominant irreversibility production mechanism and this is correlated with a decrease in the quality of cooling potential, as observed in the evolution of η_{II} for DC > 25%. It is noteworthy that within this region, the results obtained for equal duty cycles suggest that maximizing the exergy efficiency implies the use of low injection frequencies and longer pulse durations.

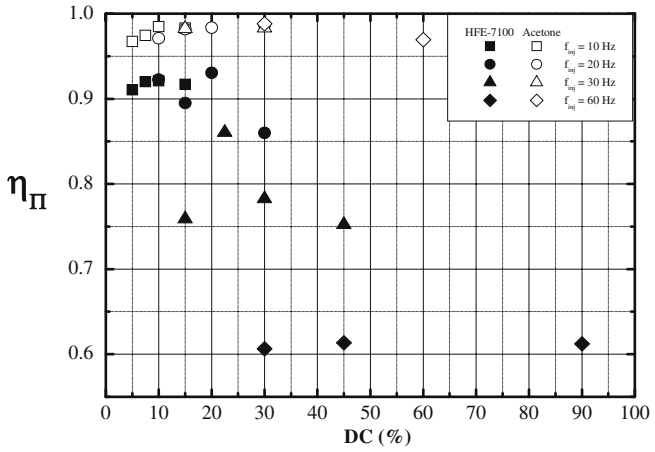

Fig. 11. Exergy efficiency as function of the duty cycle (DC) for HFE-7100 and acetone.

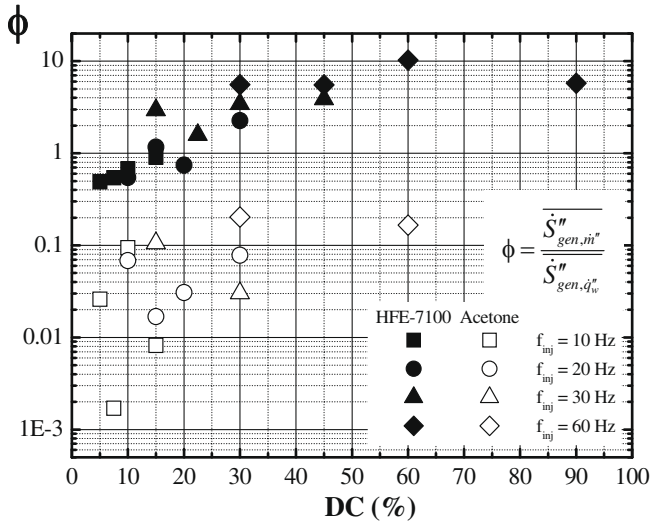

Fig. 12. Irreversibility distribution ratio for the study cases relatively to the influence of proper matching the frequency with the duration of injection through the duty cycle (DC) for HFE-7100 and acetone.

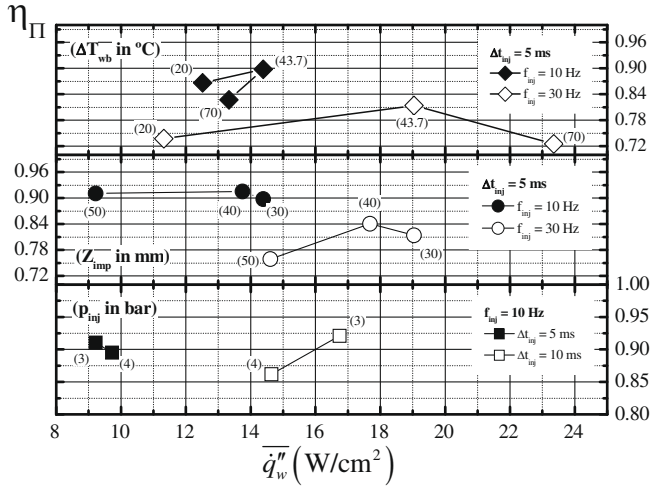

Fig. 13. Influence of superheating degree (ΔT_{wb}), impingement distance (Z_{imp}) and pressure of injection (p_{inj}) on the local exergetic efficiency for HFE-7100.

The joint analysis of energy and exergy efficiencies shows that HFE-7100 and acetone have similar behaviors in the energy efficiency as function of DC, but acetone is able to keep a minimum destruction of exergy compared with HFE-7100. It is here that the irreversibility distribution ratio could be useful to interpret these differences between fluids. In light of Fig. 12, the value of ϕ obtained for acetone remains below 1, regardless of DC, suggesting that irreversibilities produced by mass evaporation are less important than those produced by the wall heat flux. If this is associated with an effect of the latent heat of evaporation, it would explain why phase-change still being promoted in the case of acetone, while mitigated in the case of HFE-7100. In fact, an additional key point when the cooling liquid changes from HFE-7100 to acetone, is the latent heat of evaporation, which increases substantially in the later. The fact that irreversibilities produced by the wall heat flux are more important in acetone experiments, compared with HFE-7100, could be associated with this difference in the latent heat of evaporation. What is noteworthy in this comparison is that promoting phase-change implies the highest possible quality of the cooling potential and suggests the importance of the latent heat of evaporation in the design of an ISC system.

The results depicted in Figs. 9–11 should also be interpreted in light of the heat transfer mechanisms enabling the cooling process. The identification of these has been previously reported for intermittent spray cooling experiments in Moreira and Panão (2006). At lower injection frequencies, phase-change was already identified as the dominant heat transfer mechanism. However, by decreasing the time interval between consecutive injections, a greater interaction between injection events result in the formation of a liquid film (see Fig. 5). Consequently, the cooling system begins extracting heat through in a different mechanism and, instead of promoting phase-change, high heat flux extraction is dominated by a *thin film boiling* based mechanism, as described by Kopchikov et al. (1969) and identified in previous experiments considering the whole impact area (Moreira and Panão, 2006). What justifies the high heat fluxes in this mechanism is described by Pais et al. (1992) as the piercing of cooler liquid droplets upon the film, eventually reaching the surface and enhancing the cooling process. In such mechanism, visualized in Fig. 5 for an injection frequency of 60 Hz, heat is conducted through the film instead of being used to vaporize it, which mitigates phase-change, but not suppresses it and, consequently, leads to a decrease in the spray cooling efficiency.

It is worth summarizing at this point that, while with low injection frequencies and short duty cycles, the heat transfer is mainly dominated by phase-change, if a faster thermal response is required from the system, larger duty cycles should be used, although at the cost of the system's energetic efficiency. The changes in the system's efficiency as DC approaches the continuous spray working condition (DC = 100%) could be attributed to a switching between heat transfer mechanisms, i.e. from one based on phase-change to another based on thin film boiling. Furthermore, the comparison between the dielectric fluid (HFE-7100) and acetone also suggests that a higher latent heat of evaporation is important to keep the destruction of exergy minimal and maintain the quality of the cooling potential. Ultimately, is should be remarked that the benefit retrieved from the combination of two heat transfer mechanisms in a ISC system – phase-change using the spray intermittency and thin film boiling as in continuous spray cooling (DC → 100%) – is to confer adaptability and versatility to the cooling system, additionally with the possibility of a real-time active control of the cooling process. So far, the analysis has focus on the influence of the duty cycle on heat transfer, however, as mentioned in the introduction, other parameters are relevant in the spray cooling process. The next section addresses a preliminary parametric study of that relevance.

3.4. Effect of superheating degree, impingement distance and pressure of injection

A series of experiments were devised to perform a preliminary study on the influence of the superheating degree ($\Delta T_{wb} = T_w - T_b$), the impingement distance and the pressure of injection in the ISC system's performance. According to Panão and Moreira (2005), local boiling curves (which express the transition between heat transfer regimes according to the classical boiling theory) in impinging intermittent sprays can vary locally with the injection frequency. Therefore, while the results for the exergy efficiency η_π at $f_{inj} = 10$ Hz, depicted on the top plot of Fig. 13, show a system working close to its critical heat flux (CHF), when the injection frequency increases to 30 Hz, the regime changes and the working condition is clearly in a nucleate boiling regime ($0 \leqslant \Delta T_{wb} \leqslant \Delta T_{wb}^{CHF}$). Since the pulse duration is kept constant, the highest frequency also represents a larger duty cycle, and, consequently, a higher overall cooling mass flux and the likely formation of a thin liquid film. The alteration of the surface condition at spray impact could be the reason for altering the heat transfer regime, enabling the removal of more heat, although with a lower performance. However, this point should be further investigated in future work. Moreover, following the superheating degree criterion in Eq. (21), it is noteworthy that any deviations from $\Delta T_{wb} = 43.7$ °C, for which $T_f = 22$ °C minimizes the irreversibilities produced by the heat flux extracted by the spray from the wall, have a negative impact on the exergy efficiency, independently of the heat transfer regime. This emphasizes the importance of using this criterion in the technical design of spray cooling systems.

The effect of the impingement distance on the exergy efficiency is negligible when the time lag between consecutive injections is sufficiently large (10 Hz). But as this time lag decreases (30 Hz), slight improvements are observed in exergy losses as the impinging spray approaches the wall.

The results for an increase of the injection pressure generally represent a loss in the exergy efficiency (bottom of Fig. 13), particularly accentuated with longer injection pulses (10 ms) and apart from the differences observed relatively to the time-average wall heat flux in both cases. A possible interpretation for this result is to associate the destruction of exergy with the spray impact momentum, proportional to the increase of the injection pressure. In Panão and Moreira (2005), the effect of increasing the injection pressure (spray impact momentum) was to locally decrease the wall heat flux. Considering that this effect is less important with short pulses (5 ms), the fact that less heat is extracted in the 10 ms case could imply that irreversibilities produced by the evaporation of mass become more important. To confirm this hypothesis we analyzed the irreversibility distribution ratio (ϕ) in both cases. The ϕ-value with a 5 ms injection pulse increases from 0.5 to 0.7, when the pressure increases from 3 to 4 bar, respectively, and in the case of the 10 ms injection pulse, ϕ is doubled from 0.67 to 1.4. This means that increasing the injection pressure leads to a greater dominance of the irreversibility production mechanism associated with the evaporation of mass and justifies the lower exergy efficiency.

In summary, the overall outcome of this preliminary parametric study is that a better performance of an ISC system may depend on: (i) working at superheating degrees established according to $\Delta T_{wb,opt} = 2T_f$; (ii) shorter impingement distances and; (iii) using lower injection pressures as long as a spray is produced. However, more experimental conditions are required in future work to improve our understanding of the influence exerted by each of these parameters toward the application of this new thermal management concept in micro-cooling applications.

3.5. Comparison between the ISC technological concept and other spray cooling concepts based on continuous sprays

One of the noteworthy remarks derived from the analysis in Section 3.3 is that an increase of the volumetric flux of impinging droplets (here proportional to the duty cycle) jeopardizes the evaporation efficiency, which is consistent with the results reported by other authors for continuous sprays, e.g. in Estes and Mudawar (1995), Chen et al. (2004) or Rybicki and Mudawar (2006). However, according to the analysis based on the second-law of thermodynamics performed in this work, lower energetic efficiencies does not necessarily mean lower quality in that energy transfer (see our analysis on the results for acetone in Section 3.3), therefore, this confirms the importance of taking into account the information provided by an exergy analysis for a more accurate interpretation of the spray cooling performance.

In this section, a comparison is made between this new concept and experiments with continuous sprays. The results with continuous sprays considered were obtained by Estes and Mudawar (1995) and Pautsch and Shedd (2005) with FC-72, and are compared with the HFE-7100 experiments, since these are similar fluids from the same manufacturer and have the same applicability domain. The expression for the energy efficiency in this comparison does not consider the term associated with the sensible heat in order to match the energy efficiency definition used by the other authors, and the mass flux considers only incoming drops impinging on the wall, thus $\eta_I' = \dot{\overline{q}}_w'' / (G_{in} \cdot h_{fg})$.

A preliminary step in this comparison is to correlate the energy efficiency in the experiments reported here, with the mass flux impinging on the wall. These results are summarized in Fig. 14, including the correlation obtained.

The following step is to estimate the mass flux that would be used in the ISC technological concept to match the energetic efficiency reported in the cases used for comparison. Finally, the comparison is made between the energy efficiency and the liquid saving achieved by ISC (see Fig. 15). The results show that for efficiencies between 10% and 45%, an ISC system may save 10–90% of the liquid used for cooling, which confirms the promising potential of using intermittent sprays as a new thermal management technology.

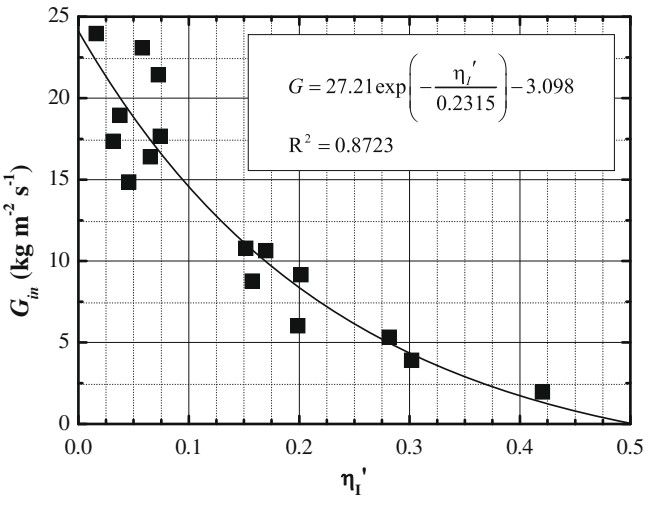

Fig. 14. Correlation between the energy efficiency and the mass flux os fluid deposited on the surface for experiments with HFE-7100.

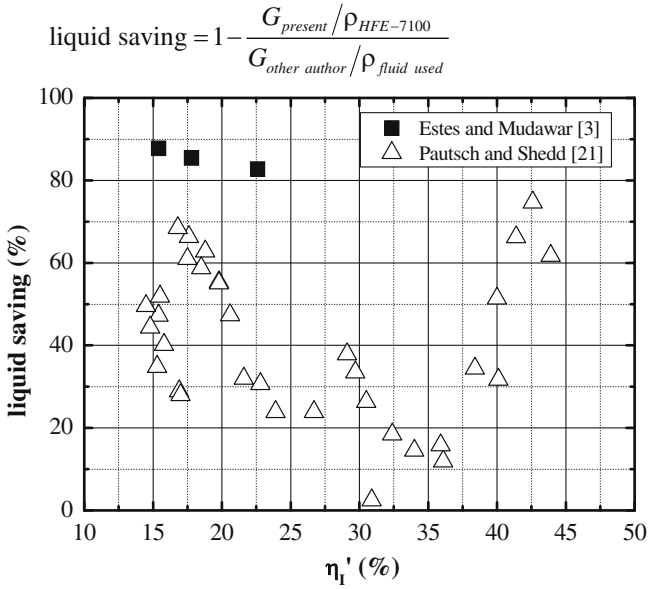

Fig. 15. Comparison between intermittent spray cooling and other spray cooling using continuous sprays in terms of the relation between liquid savings for equal energy efficiencies.

4. Conclusions

In the work presented here, intermittent spray cooling is proposed as a new technological concept for removing heat fluxes with good performance, ensuring the best quality possible in its cooling potential, and enabling the potential future application of advanced control techniques in the development of thermal management systems. In intermittent spray cooling, the "duty cycle" has been identified as the dominant parameter enabling the establishment of a practical interface between the physical cooling event and advanced intelligent control strategies, such as neural networks. An intermittent spray cooling system has the joint capability of removing heat by promoting phase-change at lower duty cycles, and through a thin film boiling mechanism as the duty cycle approaches the working condition of a continuous spray.

The results reported here allow the outline of general guidelines for the design of a thermal management system based on intermittent spray cooling:

- Use small duty cycles for a finer control of the surface temperature.
- Use large duty cycles for fast thermal response.
- Follow the criterion $\Delta T_{wb,\mathrm{opt}} = 2T_f$ in the choice of the cooling liquid.
- Use shorter impingement distances and low injection pressures.

A comparison is made between intermittent spray cooling and continuous sprays. The results suggest the potential of saving 10–90% of the liquid used for cooling with efficiency values similar to those reported for continuous sprays.

Acknowledgements

The authors would like to acknowledge the Foundation for Science and Technology in Portugal for the financial support through project CRYSCO-POCI/EME/57944/2004 and for financially supporting M.R.O. Panão through scholarship SFRH/BD/18669/2004.

Appendix A.1. Details on the calculation of the exergy efficiency

Taking the specific exergy for the liquid and vapor phases as

$$\begin{cases} ex_L = h_L - h_{L,T_0} - T_0(s_L - s_{L,T_0}) \\ ex_V = h_V - h_{V,T_0} - T_0(s_V - s_{V,T_0}) \end{cases} \quad (A1)$$

while $E\dot{x}''_{\mathrm{in}}$ in Eq. (25) is given by $\left(1 - \frac{T_0}{T_w}\right)\dot{q}''_w + \dot{m}''_{\mathrm{in}} ex_{\mathrm{in}}$,it is necessary to deduce $\frac{\mathrm{D}Ex''}{\mathrm{D}t}$ for determining the exergy entropy η_Π. This deduction begins by considering the canonical relation for exergy as $\mathrm{d}ex = \mathrm{d}h - T_0\mathrm{d}s$ in its material derivative form (D/Dt)

$$\frac{\mathrm{D}ex}{\mathrm{D}t} = \frac{\mathrm{D}h}{\mathrm{D}t} - T_0\frac{\mathrm{D}s}{\mathrm{D}t} \quad (A2)$$

If the volumetric exergy Ex''' is expressed as $\rho \cdot ex$, its material derivative in respect to the specific exergy becomes

$$\rho\frac{\mathrm{D}ex}{\mathrm{D}t} = \frac{1}{h_f}\frac{\mathrm{D}Ex''}{\mathrm{D}t} - \frac{(1-\chi)ex}{h_f}\frac{\mathrm{D}m''}{\mathrm{D}t} \quad (A3)$$

using a similar mathematical procedure as when Eq. (17) was obtained. Applying Eqs. (16) and (A3) in (A2), the exergy flux is expressed as

$$\frac{\mathrm{D}Ex''}{\mathrm{D}t} = \rho h_f\frac{\mathrm{D}h}{\mathrm{D}t} + (1-\chi)ex\frac{\mathrm{D}m''}{\mathrm{D}t} - \frac{T_0}{T_{LF}}\dot{q}''_w \quad (A4)$$

In Eq. (A4), expressing the relation $\mathrm{d}h = c_p\mathrm{d}T$ in its material derivative form as $\frac{\mathrm{D}h}{\mathrm{D}t} = c_p\frac{\mathrm{D}T}{\mathrm{D}t}$, and assuming that temperature gradients inside the liquid film are negligible, DT/Dt can be simplified to $\partial T/\partial t$. Following this, considering the energy equation for heat conduction inside the film, $c_p\frac{\partial T}{\partial t} = \frac{1}{\rho}\frac{\partial \dot{q}''}{\partial z}$, plus Eq. (15) results in the simplification the first term on the right hand side of Eq. (A4) which becomes equal to the wall heat flux $\dot{q}''_w$. Taking ex as $[\chi ex_V + (1\text{-}\chi)ex_L]$ in Eq. (A4) and integrating over the arbitrary range of χ, it simplifies into

$$\frac{\mathrm{D}Ex''}{\mathrm{D}t} = \frac{1}{12}(3ex_V + 5ex_L)\Delta\dot{m}'' + \left(1 - \frac{T_0}{T_{LF}}\right)\dot{q}''_w \quad (A5)$$

References

Arcoumanis, C., Chang, J.-C., 1993. Heat transfer between a heated plate and an impinging transient diesel spray. Experiments in Fluids 16, 105–119.
Bejan, A., 1996. Entropy generation minimization: the new thermodynamics of finite-size devices and finite-time processes. Journal of Applied Physics 79, 1191–1218.
Cader, T., Westra, L.J., Eden, R.C., 2004. Spray cooling thermal management for increased device reliability. IEEE Transactions on Device and Mat Reliability 4, 605–613.
Chen, R.-H., Chow, L.C., Navedo, J.E., 2004. Optimal spray characteristics in water spray cooling. International Journal of Heat and Mass Transfer 47, 5095–5099.
Chen, X.D., Nguang, S.K., 2003. The theoretical basis of heat flux sensor. Journal of Applied Mathematics and Decision Sciences 7, 1–10.
Estes, K.A., Mudawar, I., 1995. Correlation of Sauter mean diameter and critical heat flux for spray cooling of small surfaces. International Journal of Heat and Mass Transfer 38, 2985–2996.
Kopchikov, I., Voronin, G., Kolach, T., Labuntsov, D., Lebedev, P., 1969. Liquid boiling in a thin film. International Journal of Heat and Mass Transfer 12, 791–796.
Loureiro, H., Panão, M.R.O., Moreira, A.L.N., 2004. Simultaneous measurements of droplet characteristics and surface thermal behavior to study spray cooling with pulsed sprays. In: Twelfth International Symposium on Applications of Laser Techniques to Fluid Mechanics, Lisbon, Portugal.
Majaron, B., Svaasand, L.O., Aguilar, G., Nelson, J.S., 2002. Intermittent cryogen spray cooling for optimal heat extraction during dermatologic laser treatment. Physics in Medicine and Biology 47, 3275–3288.
Moita, A.S., Moreira, A.L.N., 2007. Characterization of hydrodynamics and heat-transfer processes of drop impacts against surface enhanced heated targets as an application to microelectromechanical cooling devices. In: International Conference on Multiphase Flow, ICMF-2007, Leipzig, Germany.
Moreira, A.L.N., Panão, M.R.O., 2006. Heat transfer at multiple-intermittent impact of a hollow cone spray. International Journal of Heat and Mass Transfer 49, 4132–4151.
Moreira, A.L.N., Carvalho, J., Panão, M.R.O., 2007. An experimental methodology to quantify the spray cooling event at intermittent spray impact. International Journal of Heat and Fluid Flow 28, 191–202.

Pais, M.R., Chow, L.C., Mahefkey, E.T., 1992. Surface roughness and its effects on the heat transfer mechanism in spray cooling. Journal of Heat Transfer 114, 211–219.

Panão, M.R.O., Moreira, A.L.N., 2004. Experimental study of the flow regimes resulting from the impact of an intermittent gasoline spray. Experiments in Fluids 37, 834–855.

Panão, M.R.O., Moreira, A.L.N., 2005. Thermo- and fluid dynamic characteristics of spray cooling with pulsed sprays. Experimental Thermal and Fluid Science 30, 79–96.

Panão, M.R.O., Moreira, A.L.N., 2006. Two-phase cooling characteristics of a multiple-intermittent spray. In: Thirteenth International Symposium on Applications of Laser Techniques to Fluid Mechanics, Lisbon, Portugal.

Pautsch, A.G., Shedd, T.A., 2005. Spray impingement cooling with single- and multiple-nozzle arrays. Part: I Heat transfer data using FC-72. International Journal of Heat and Mass Transfer 48, 3167–3175.

Reichelt, L., Meingast, U., Renz, U., 2002. Calculating transient wall heat flux from measurements of surface temperature. International Journal of Heat and Mass Transfer 45, 579–584.

Reid, R.C., Prausnitz, J.M., Poling, B.E., 1986. The Properties of Gases and Liquids. McGraw-Hill, New York.

Roisman, I.V., Tropea, C., 2001. Flux measurements in sprays using phase-Doppler techniques. Atomization and Sprays 11, 667–700.

Rybicki, J.R., Mudawar, I., 2006. Single-phase and two-phase cooling characteristics of upward-facing and downward-facing sprays. International Journal of Heat and Mass Transfer 49, 5–16.

Schultz, D.L., Jones, T.V., 1973. Heat Transfer Measurements in Short-Duration Hypersonic Facilities. AGARD-AG-165 5, p. 84.

Shedd, T.A., Pautsch, A.G., 2005. Spray impingement cooling with single- and multiple-nozzle arrays. Part II: Visualization and empirical models. International Journal of Heat and Mass Transfer 48, 3176–3184.

Yao, S.C., Choi, K.J., 1987. Heat transfer experiments of mono-dispersed vertically impacting sprays. International Journal of Heat and Mass Transfer 13, 639–648.